Spindle checkpoint activation at meiosis I advances anaphase II onset via meiosis-specific APC/C regulation

Ayumu Yamamoto,[1,2] Kenji Kitamura,[3] Daisuke Hihara,[1] Yukinobu Hirose,[1] Satoshi Katsuyama,[1] and Yasushi Hiraoka[2]

[1]Department of Chemistry, Shizuoka University, Suruga-ku, Shizuoka 422-8529, Japan
[2]Cell Biology Group, Kansai Advanced Research Center, National Institute of Information and Communications Technology, Nishi-ku, Kobe 651-2492, Japan
[3]Center for Gene Science, Hiroshima University, Higashi Hiroshima 739-8527, Japan

During mitosis, the spindle assembly checkpoint (SAC) inhibits the Cdc20-activated anaphase-promoting complex/cyclosome (APC/C^{Cdc20}), which promotes protein degradation, and delays anaphase onset to ensure accurate chromosome segregation. However, the SAC function in meiotic anaphase regulation is poorly understood. Here, we examined the SAC function in fission yeast meiosis. As in mitosis, a SAC factor, Mad2, delayed anaphase onset via Slp1 (fission yeast Cdc20) when chromosomes attach to the spindle improperly. However, when the SAC delayed anaphase I, the interval between meiosis I and II shortened. Furthermore, anaphase onset was advanced and the SAC effect was reduced at meiosis II. The advancement of anaphase onset depended on a meiosis-specific, Cdc20-related factor, Fzr1/Mfr1, which contributed to anaphase cyclin decline and anaphase onset and was inefficiently inhibited by the SAC. Our findings show that impacts of SAC activation are not confined to a single division at meiosis due to meiosis-specific APC/C regulation, which has probably been evolved for execution of two meiotic divisions.

Introduction

Meiosis is a special type of cell division that generates haploid gametes from diploid progenitors. During meiosis, two rounds of chromosome segregation successively take place without an intervening S phase. At meiosis I (MI), homologues segregate apart from each other (reductional segregation), whereas at meiosis II (MII), sister chromatids segregate apart from each other (equational segregation). These distinct types of chromosome segregation depend on distinct types of spindle attachment of chromosomes: at MI, homologues attach to the opposite spindle poles (bipolar attachment), whereas sister chromatids attach to the same pole (monopolar attachment); in contrast, at MII, sister chromatids attach to the opposite poles. How these distinct types of attachment are properly established is one of the fundamental problems in meiosis.

It is thought that the spindle assembly checkpoint (SAC) ensures proper spindle attachments of chromosomes. Chromosomes attach to the spindle via a special site called the kinetochore, and the spindle–kinetochore interaction is stabilized by tension generated at the kinetochore. The SAC delays anaphase onset by sensing unattached kinetochores and/or a lack of tension. This delay provides time for the cells to correct the improper attachments, thereby ensuring accurate chromosome segregation (Musacchio and Hardwick, 2002).

The SAC inhibits anaphase promoting complex/cyclosome (APC/C), an E3 ubiquitin ligase that promotes proteasome-dependent protein degradation and induces anaphase. During mitosis, APC/C is activated by two related factors, Cdc20/Slp1/Fzzy and Cdh1/Ste9/srw1/Fzzy-related (for review see Peters, 2006). Cdc20-activated APC/C (APC/C^{Cdc20}) first initiates anaphase onset by promoting the degradation of B-type cyclin and securin (e. g., Cut2 in fission yeast [Funabiki et al., 1996] and Pds1 in budding yeast [Cohen-Fix et al., 1996; Yamamoto et al., 1996]). Cyclin B degradation causes the decline of the

Correspondence to Ayuma Yamamoto: sayamam@ipc.shizuoka.ac.jp

Abbreviations used in this paper: APC/C, anaphase promoting complex/cyclosome; MI, meiosis I; MII, meiosis II; SAC, spindle assembly checkpoint; SPB, spindle pole body.

The online version of this paper contains supplemental material.

The Rockefeller University Press $30.00
J. Cell Biol. Vol. 182 No. 2 277–288
www.jcb.org/cgi/doi/10.1083/jcb.200802053

Cdk activity, whereas securin degradation liberates separase, which resolves sister chromatid cohesion and activates the FEAR pathway that also regulates anaphase events (D'Amours and Amon, 2004). After APC/C^{Cdc20} initiates anaphase, APC/C^{Cdh1} facilitates exit from mitosis by degrading additional APC/C substrates and maintains the low level of cyclin B during the next G1 phase. It has been shown in mitosis that the SAC targets APC/C^{Cdc20}. Mad2, one of the best-characterized SAC factors, directly binds to Cdc20 to inhibit the APC/C^{Cdc20} activity (Musacchio and Hardwick, 2002). Mad2 binding is thought to be stimulated by kinetochores that fail to attach to the spindle, as Mad2 accumulates at unattached kinetochores, which generate signals to delay anaphase onset.

At meiosis, the SAC probably delays anaphase onset, as in mitosis, but meiotic SAC functions are not fully understood. Direct observation of chromosomes in insects showed that the SAC delays chromosome segregation at MI (Nicklas, 1997), and previous studies of recombination-defective mutants of budding and fission yeasts showed that when tension is not generated at the kinetochore, the SAC induces a delay at MI (Shonn et al., 2000; Yamaguchi et al., 2003). However, it has never been shown in any organisms that the SAC delays anaphase II onset.

Moreover, impacts of SAC activation may differ at meiosis. Anaphase regulation has been shown to be different at meiosis. Studies in frogs showed that APC/C does not fully degrade cyclin at the end of the first division so that the Cdk activity is retained at an intermediate level at the MI–MII transition, which leads to initiation of MII without starting DNA replication (Iwabuchi et al., 2000). Consistently, meiosis-specific factors regulate APC/C. In fission yeast, a meiosis-specific APC/C activator, Fzr1, is required for proper sporulation (Asakawa et al., 2001; Blanco et al., 2001), and Mes1, a meiosis-specific inhibitor of APC/C^{slp1}, is required for initiation of MII (Izawa et al., 2005). In budding yeast, Ama1, a putative functional homologue of Fzr1, is required for proper execution of MI and subsequent sporulation (Cooper et al., 2000; Oelschlaegel et al., 2005; Penkner et al., 2005). A meiosis-specific APC/C activator also plays a critical role in meiotic anaphase in *Drosophila melanogaster* (Jacobs et al., 2002). Meiosis-specific anaphase regulation raises the possibility that SAC activation causes different consequences at meiosis.

In this study, we sought to elucidate the precise regulatory function of the SAC in the progression of meiosis by observing meiotic events in living fission yeast cells. We show that the SAC delays anaphase onset not only at MI but also at MII. We further show that impacts of SAC activation are not confined to a single division at meiosis because of meiosis-specific regulation of APC/C, which has probably been evolved for execution of two consecutive meiotic divisions.

Results

Dynamics of the spindle, the chromosome, and cyclin B during meiotic divisions in wild-type cells

As a first step toward understanding the SAC function in meiotic anaphase regulation, we characterized meiotic events in wild-type fission yeast cells. Conventional analysis of fixed specimens of cultures synchronously induced to enter meiosis was not suitable for characterization because of poor synchronization of the cultures and the rapid progression of meiosis. To circumvent this problem, we examined the dynamics of the spindle and the chromosome three-dimensionally in individual living cells. Visualization of the spindle using GFP-tagged α2-tubulin showed three distinct phases in spindle elongation at both divisions, as seen in mitosis (Fig. 1, A and B; Nabeshima et al., 1998). A short spindle forms in the first phase (Fig. 1, A and B, PI) and remains relatively constant in length in the second phase (PII); the spindle further elongates and eventually disappears in the third phase (PIII). At MII, the two spindles elongated synchronously with almost identical kinetics (Fig. 1 B, right). The behavior of the MI spindle was consistent with that described by Yamaguchi et al. (2003).

We next examined the chromosome dynamics in relation to the spindle dynamics. We visualized several chromosome loci using the lac operator/repressor GFP tagging system (Fig. 1 C; Yamamoto and Hiraoka, 2003; Ding et al., 2004) and the spindle pole body (SPB) using the GFP-tagged SPB component Sid4 (Tomlin et al., 2002). The GFP-visualized chromosomal loci and spindle poles were distinguished by their distinct signal intensity and behavior. Visualization of centromeres of chromosome II (*cen2*) showed that in half of the cases (4 out of 8), the centromeres were located near the SPB before spindle formation at MI (Fig. 1 D, PI, 0 min). In the rest of the cases, the centromeres were located away from the SPB (Fig. 1 E, 0 min). Regardless of the initial centromere positions, pairs of homologous centromeres became located between the two poles during phase I (Fig. 1, D, 6 min; and Fig. 1, E, 8 min) and, subsequently, coordinately oscillated with a relatively constant distance between the two poles until the end of phase II (Fig. 1 D, PII; Fig. 1 D, right, D1 and D2; and Table S2, available at http://www.jcb.org/cgi/content/full/jcb.200802053/DC1). Thus, homologues attach to both spindle poles during spindle formation and experience opposing forces from the spindle, and phase II probably corresponds to metaphase in higher eukaryotes, during which chromosomes oscillate coordinately between the spindle poles at the spindle equator (Skibbens et al., 1993). The distances between the homologous centromeres during phase II appeared to vary among cells, perhaps reflecting different chromosomal positions of the chiasma that links homologues; the further away the chiasma is from the centromere, the further apart centromeres are pulled. At the end of phase II, the homologous centromeres separated from each other to reach the opposite poles (Fig. 1 D, 25 min) and further separated during phase III with the elongating spindle (Fig. 1 D, PIII). Thus, homologues sequentially undergo anaphase A and anaphase B during reductional segregation. Simultaneous visualization of different centromere-linked loci (Fig. 1 C, *cen2* and *lys1*) showed that different chromosomes undergo anaphase almost concomitantly (not depicted). Sister centromeres mostly remained associated with each other throughout MI, as shown by rare splitting into two of the *cen2* dots (3.9% of observed events). In contrast, sister chromatid arms separated around anaphase onset (Fig. 1 F, 21 min). This is consistent with the idea that sister chromatid arm separation causes resolution of the chiasma and

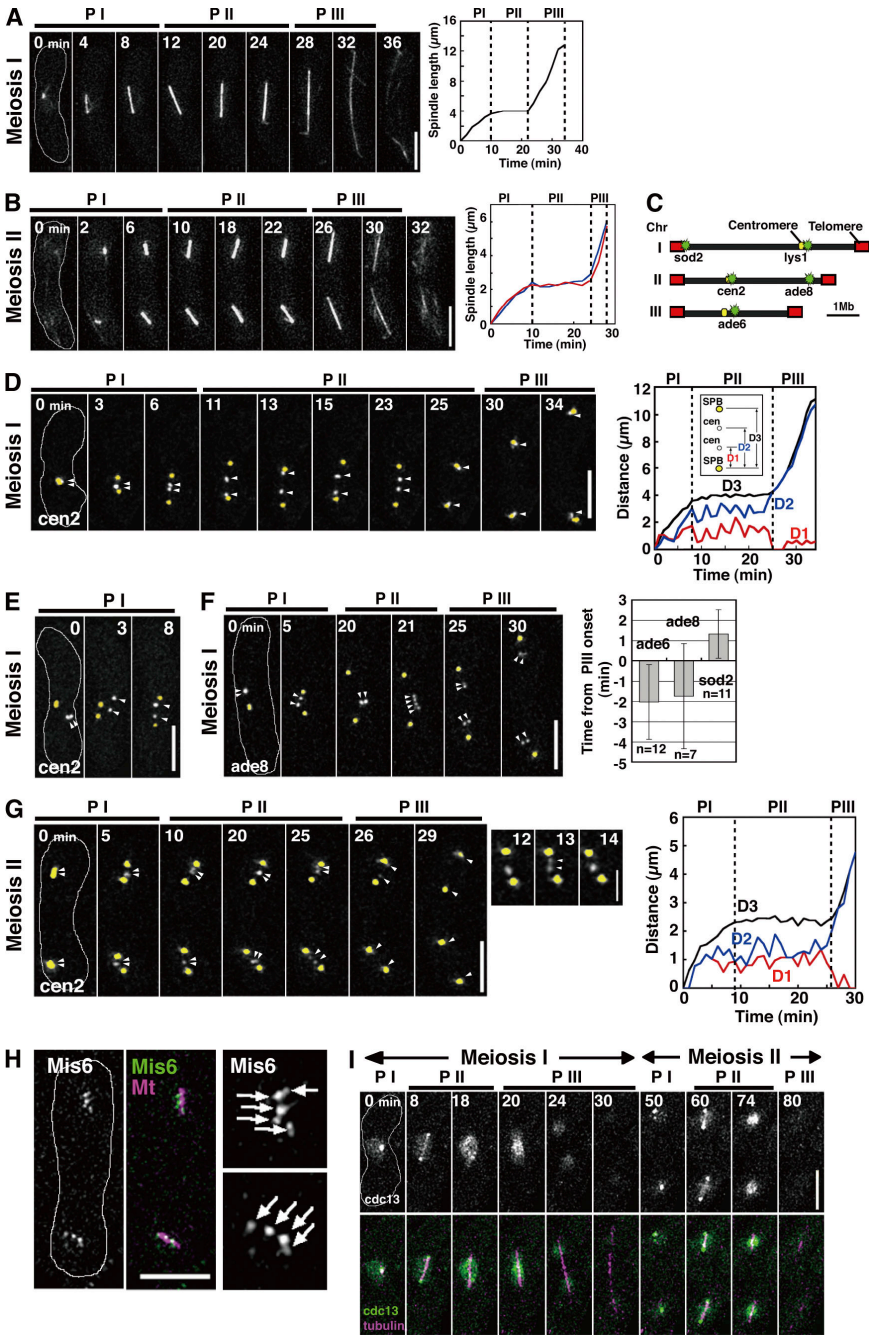

Figure 1. **Dynamics of the spindle, the chromosome, and Cdc13 at meiosis in the wild type.** (A and B) Spindle behavior at MI and MII. Graphs show changes in spindle length. In the graph in B, lengths of the two MII spindles are shown as blue and red lines. (C) An approximate map of GFP-visualized loci on three chromosomes used in this study. (D and E) Behavior of homologous centromeres (*cen2*; white, arrowheads) and the SPB (yellow) at MI. The graph shows changes in distance between two SPBs (D3) and between one of the SPBs and each centromere (D1 and D2). (F) Behavior of the arm locus (*ade8*; bottom, white, arrowheads, and graph) and the SPB (yellow) at MI. The graph shows the mean time of sister locus separation. Time 0 is PIII onset. (G) Behavior of sister centromeres (arrowheads) at MII. Arrowheads in enlarged images highlight transient sister centromere separation before anaphase. The graph shows changes in SPB-cen (D1 and D2) and SPB-SPB (D3) distances at MII. (H) Centromeres were visualized by Mis6-GFP and the spindle was visualized by mDsRed-α2-tubulin at MII (8 min before anaphase). (right) Images are enlarged views of Mis6 dots (arrows). (I) Dynamics of Cdc13-GFP at meiosis in the wild type. White lines in images indicate cell shapes. Dotted lines in graphs show boundaries of the spindle phases. Error bars indicate standard deviation. PI, phase I; PII, phase II; PIII, phase III. Bars: (A, B, and D–H) 5 μm; (G, inset) 2 μm.

thereby dissociation of homologues (Petronczki et al., 2003). The telomere-proximal loci (*sod2*) separated slightly later than other arm loci (Fig. 1 F, right), which suggests that telomere separation occurs after arm separation.

At MII, sister chromatids were held together at centromeres, as one centromere (*cen2*) dot (Fig. 1 G, 5 min) and two arm (*ade8*) dots (not depicted) were observed for each spindle in an early stage of MII. Sister centromeres probably attach to both poles during phase I, as indicated by the *cen2* positions between the two poles. Unexpectedly, however, they frequently underwent transient dissociation at phase II, as shown by the frequent splitting of the *cen2* dot into two (Fig. 1 G, enlarged images, 13 min, arrowheads; and Fig. 1 G, right, D1 and D2). This sister centromere splitting was not caused by integration of the lac operator repeats into the chromosome because more than three GFP dots were observed when we visualized the centromeres of all three pairs of sister chromatids using GFP-tagged centromere component Mis6 (Fig. 1 H, arrows). The split sister centromeres frequently oscillated between the poles coordinately, as homologous centromeres do at MI (Table S2). Transient separation indicates that sister centromere cohesion is not strong enough to resist the opposing forces and that sister chromatid cohesion is still retained at arms. Arm cohesion, however, is probably restricted to centromere-proximal regions because the centromere-distal arm loci (*ade8*) remained separated throughout MII (not depicted). Sister chromatids eventually underwent anaphase A and anaphase B, as homologues do at MI (Fig. 1 G, PIII).

We also characterized the dynamics of cyclin B, Cdc13, which is a major substrate of APC/C and thereby a good indicator for the APC/C activity. Cdc13 tagged with GFP (Cdc13-GFP) was localized both at the spindle and throughout the nucleus at MI (Fig. 1 I, 0 and 8 min). Spindle Cdc13-GFP disappeared just before phase III (Fig. 1 I, 18 min; and Fig. S1 A, meiosis I, available at http://www.jcb.org/cgi/content/full/jcb.200802053/DC1), whereas nuclear Cdc13-GFP disappeared during the elongation (Fig. 1 I, 20–30 min). It should be noted that the disappearance of nuclear Cdc13-GFP appeared to start from the spindle poles to the spindle midzone (Fig. 1 I, 20 min), as seen in *D. melanogaster* embryos (Huang and Raff, 1999). After MI exit, Cdc13-GFP reaccumulated in the nucleus and on the SPB (Fig. 1 I, 50 min); then the MII spindle was formed, and Cdc13-GFP showed a similar behavior to that seen at MI (Fig. 1 I, 50–80 min; and Fig. S1 A, meiosis II). The observed Cdc13-GFP behavior was consistent with that described by Izawa et al. (2005) and similar to the behavior of Cdc2 kinase described by Decottignies et al. (2001).

The SAC delays anaphase I onset in *rec12* mutant

Having characterized the meiotic events in the wild type, we next examined a *rec12-152* mutant, which is defective in the formation of recombination-associated DNA double-strand breaks (Lin and Smith, 1994; Cervantes et al., 2000), to understand anaphase I regulation by the SAC in detail. In recombination mutants, chromosomes attach the spindle improperly because of the lack of chiasmata, and thereby, the SAC becomes activated at MI. Indeed, the SAC was previously found to delay anaphase I onset in a *rec7* recombination-defective mutant (Yamaguchi et al., 2003).

Analysis of the chromosome dynamics confirmed improper spindle attachment of chromosomes at MI in *rec12*. Homologous centromeres oscillated between the two poles independently of each other, with kinetic parameters similar to those in the wild type (Fig. 2 A, top, PII; Fig. 2 A, bottom; Fig. 2 A, top right, D1 and D2; and Table S2) and with frequent arrival at the poles before anaphase I (Fig. 2 A, top, 12 min; and Fig. 2 A, bottom, 16, 19, and 27 min); they frequently segregated to the same pole (3 out of 7 cases; Fig. 2 A, top, 59 min). In addition, sister centromeres occasionally underwent equational segregation (2 of 14 cases). Thus, both bipolar attachment of homologues and monopolar attachment of sister chromatids were perturbed in *rec12*.

Behavior of the spindle, the chromosome, and Cdc13-GFP showed that anaphase progression was delayed. The spindle dynamics were aberrant in the mutant. In half of the cells (9 out of 18 cells), the spindle underwent gradual elongation and sudden regression at phase II (Fig. 2 B, top left and top right, arrow); in the rest of the cells, the spindle continually elongated to reach its maximum length after phase I, leading to a lack of the three distinct phases (Fig. 2 B, bottom left and bottom right), and showed an aberrant morphology (thin spindle midzone; Fig. 2 B, bottom, arrowheads). In both cases, the lifetime of the spindle was markedly extended ($\sim$1.4 times longer on average), which indicates that MI progression was delayed in the mutant. In the cells with three distinct phases, phase II was solely extended (Fig. 2 C, *rec12*). Furthermore, irrespective of the spindle behavior, disappearance of the spindle-localized Cdc13 and arm separation occurred with delayed timings (Fig. 2, D, 28 min; Fig. 2 E; and Fig. S1 B, *rec12*). These results indicate that anaphase I onset is delayed in *rec12*.

Depletion of Mad2 showed that the delay depended on the SAC. The Mad2 depletion eliminated both the extension of phase II and the delay in arm separation (Fig. 2, C and E, *rec12 mad2*). In addition, the Mad2 depletion also restored the three distinct phases and normal spindle morphology. Thus, Mad2 induced the delay and the spindle abnormality in *rec12*. As in mitosis, Mad2 induces a delay by binding to Slp1, which plays a central role in meiotic anaphase (Fig. S2, A and B; and Fig. S3 A, available at http://www.jcb.org/cgi/content/full/jcb.200802053/DC1; Izawa et al., 2005), because the delay was markedly reduced by the *slp1-mr63* mutation (Fig. 2 C, *rec12 slp1-mr63*), which abolishes Mad2 binding (Kim et al., 1998). Furthermore, Mad2 induces delay probably by localizing at kinetochores that fail to attach to the spindle properly because Mad2 centromere localization was extended at MI in *rec12* (Fig. S3, B and C).

At MII, however, chromosome, and Cdc13 dynamics were largely normal except that the two spindles were frequently different in length (Fig. S3, E and F). The longer spindle was associated with a larger chromosomal mass (Fig. S3 G), which may mean that the spindle length depends on chromosome numbers. In summary, our analysis of *rec12* confirmed that the SAC delays anaphase I onset when chromosomes attach to the spindle improperly.

The SAC delays anaphase II onset in *rec8* and *clr4* mutants

We next examined *rec8* and *clr4* mutants to determine if the SAC delays anaphase II onset. Rec8 is a subunit of a meiotic type of cohesin protein complex that is required for sister chromatid cohesion (Watanabe and Nurse, 1999), whereas Clr4 is required for the centromere retention of Rec8 until anaphase II (Kitajima et al., 2003). In these mutants, sister chromatids are prematurely dissociated from each other and, thereby, chromosomes probably attach to the spindle improperly. If the SAC delays anaphase II onset, it should do so in the mutants.

Analysis of the chromosome dynamics confirmed premature dissociation and improper spindle attachments of sister chromatids in these mutants. In *rec8*, sister chromatids underwent equational segregation at MI (not depicted; Watanabe and Nurse, 1999) and remained separated at MII (Fig. 3 A, top, *rec8*), whereas in *clr4*, although chromosomes underwent normal segregation at MI (not depicted), sister chromatids prematurely dissociated at MII (Fig. 3 A, bottom, *clr4*). As a consequence, preanaphase sister centromere distances increased by approximately twofold on average in both mutants (Fig. 3 B). Sister centromeres oscillated between the two poles independently of each other in *rec8* (Fig. 3 A, top, *rec8*, PII; and Fig. 3 A, top right, D1 and D2), whereas they oscillated coordinately with apparent anaphase A movement thereafter in *clr4* (Fig. 3 A, bottom, *clr4*, PII; Fig. 3 A, bottom right, D1 and D2; and Table S2). Despite this difference, chromosomes attach to the spindle improperly, as shown by sister centromere segregation to the same pole (43.8% in 16 cells for *rec8* and 21.4% in 14 cells for *clr4*; Fig. 3 A, top, 34 min) and centromere lagging (37.5% for *rec8* and 25.0% for *clr4*; Fig. 3 A,

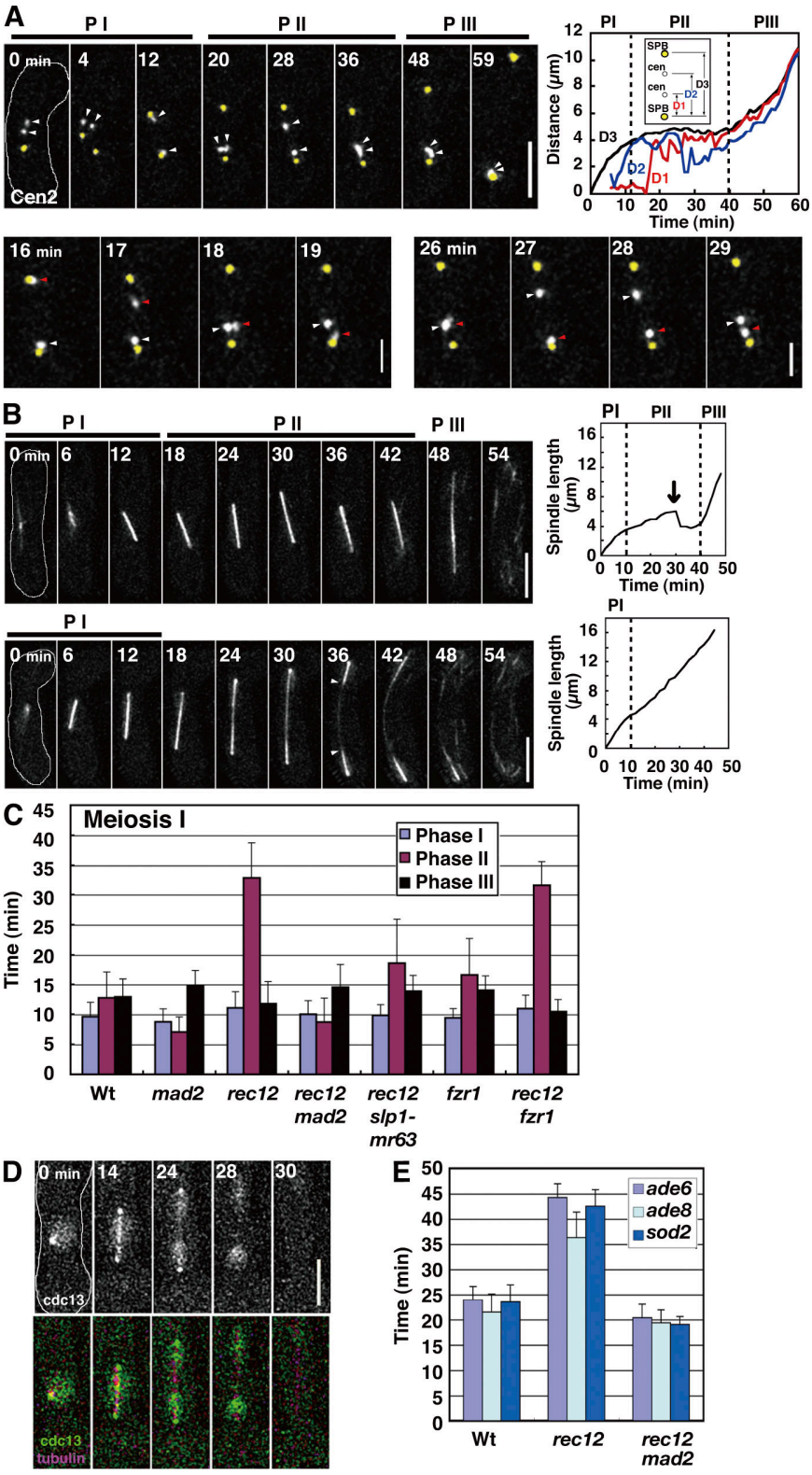

Figure 2. **Dynamics of the chromosome, the spindle, and Cdc13 at MI in *rec12* mutant.** (A) Behavior of homologous centromeres and the SPB at MI. Arrowheads indicate the homologous centromeres (*cen2*). Bottom panels highlight independent oscillations of the homologous centromeres (white and red arrowheads) at phase II. The graph shows changes in the SPB-cen (D1 and D2) and SPB-SPB (D3) distances. (B) Behavior of the MI spindle in *rec12*. The arrow in the top graph shows the sudden regression of the spindle. Arrowheads indicate the thin spindle midzone. Dotted lines in graphs show boundaries of the spindle phases. PI, phase I; PII, phase II; PIII, phase III. (C) Duration of spindle phases. (D) Dynamics of Cdc13-GFP at MI. (E) Timing of arm locus separation at MI. Bars show time of separation of the *ade6*, *ade8*, and *sod2* loci after spindle formation. At least seven cells were examined for each locus. Wt, wild type. Error bars indicate standard deviation. Bars: (A, top, B, and D) 5 μm; (A, bottom) 2 μm.

top right, *rec8*), and the parameters of centromere movements were similar (Table S2).

Analysis of the spindle, chromosome, and Cdc13 dynamics showed anaphase delay in the mutants. In *rec8*, the MII spindle prematurely elongated and regressed at phase II like the MI spindle in *rec12* (Fig. 3 C, *rec8*), but it eventually underwent a discernible phase III elongation with normal spindle morphology. In *clr4*, however, the MII spindle behaved almost normally at phase II (Fig. 3 C, *clr4*). Despite this difference, the phase II duration was significantly extended in both mutants (Fig. 3 D, *rec8* and *clr4*). Consistently, in *rec8*, Cdc13 disappeared from the spindle with significant delay (Fig. S1 B, *rec8*), and in *clr4*,

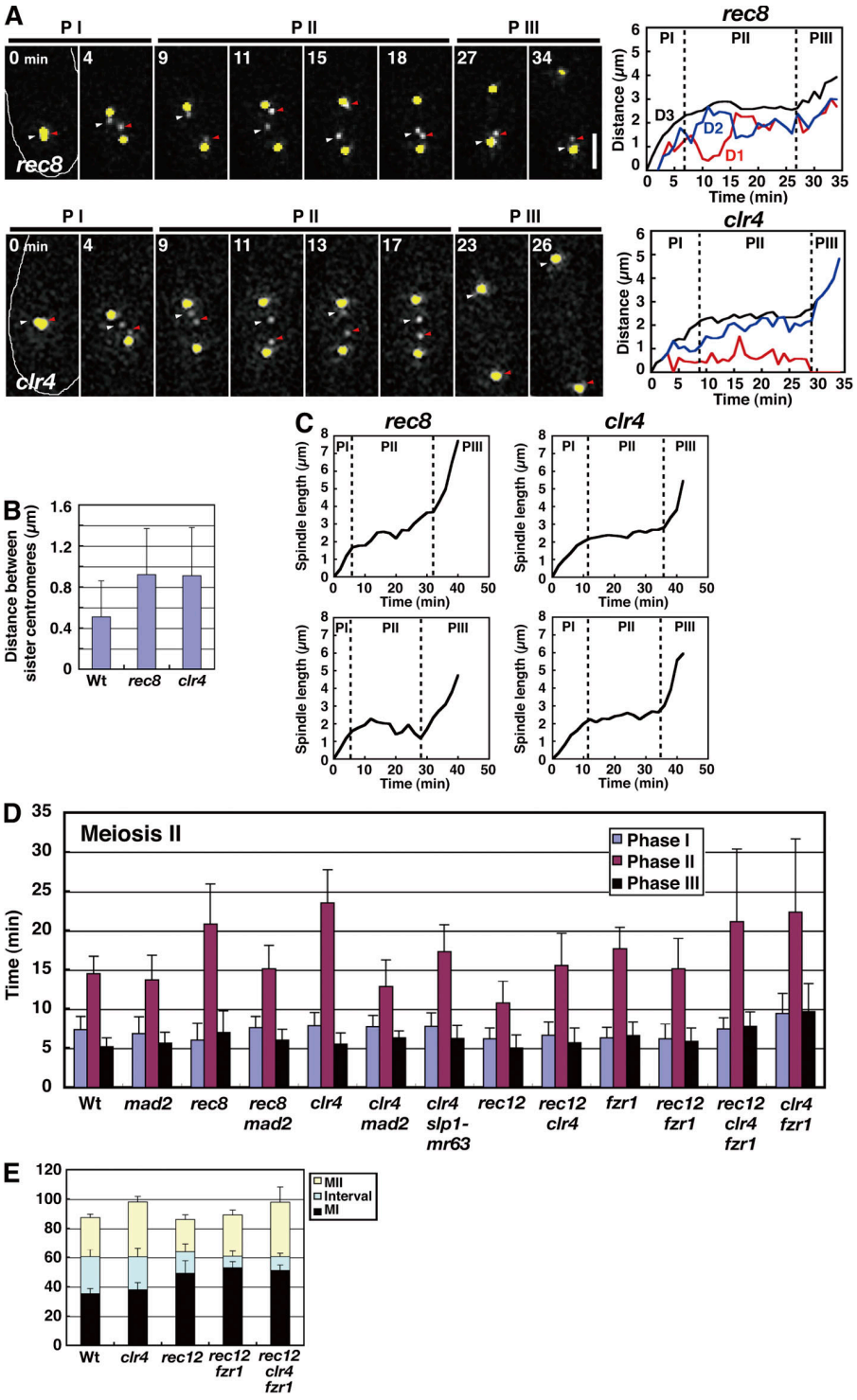

Figure 3. **Dynamics of the chromosome and the spindle at MII in *rec8* and *clr4* mutants.** (A) Behavior of sister centromeres (white and red arrowheads) and the SPB (yellow) at MII in *rec8* (top left and right) and *clr4* (bottom left and right) mutants. The graph shows changes in the SPB-cen (D1 and D2) and SPB-SPB (D3) distances. PI, phase I; PII, phase II; PIII, phase III. Bar, 2 μm. (B) Mean distances of centromeres at phase II. More than eight pairs of centromeres were examined for each analysis. (C) Changes in spindle length at MII in the *rec8* (left) and *clr4* (right) mutants. Graphs show kinetics of two MII spindles in the same cell. Dotted lines in graphs show boundaries of the spindle phases. (D) Duration of the spindle phases at MII. (E) Duration of MI, MII, and the MI–MII interval. Wt, wild type. Error bars indicate standard deviation.

anaphase A started with delayed timing (14.9 ± 3.8 min for the wild type [n = 22] but 18.9 ± 2.6 min after the start of phase II for *clr4* [n = 15]). These results indicate that anaphase II onset was delayed in both mutants.

As seen at MI in the *rec12* mutant, the Mad2 depletion and *slp1-mr63* mutation eliminated the delay (Fig. 3 D, *rec8 mad2*, *clr4 mad2*, and *clr4 slp1-mr63*). Therefore, Mad2 delays anaphase II onset via Slp1. It should be noted that two MII spindles sometimes started anaphase spindle elongation at different times (Fig. 3 C, *rec8*), which suggests that the SAC regulates two MII divisions independently of each other in the same cell. Collectively, we concluded that the SAC delays anaphase II onset when chromosomes improperly attach to the spindle.

Anaphase I delay causes advancement of anaphase II onset

We examined if the SAC activation causes any other impacts on the progression of meiosis. We noticed that the interval between

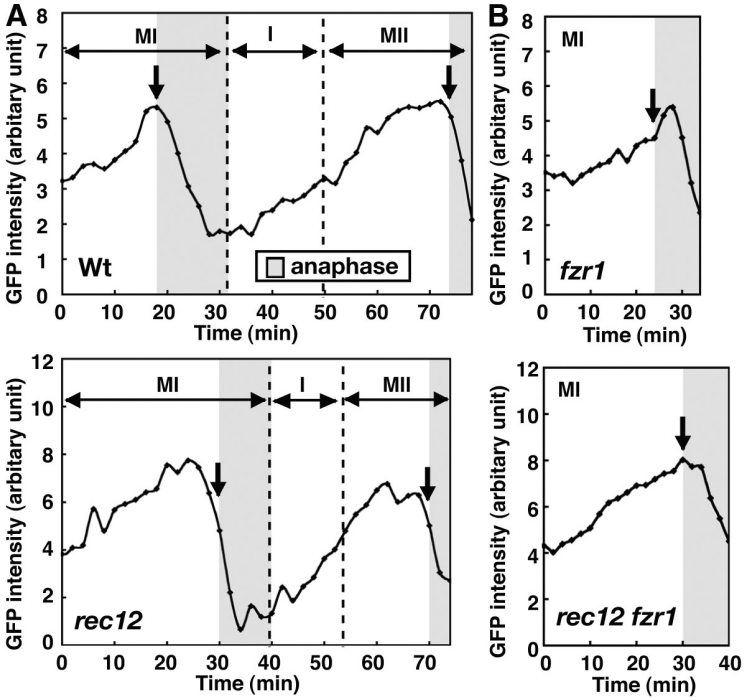

Figure 4. **Changes in the amount of nuclear Cdc13.** (A) Changes in Cdc13-GFP amount in the nucleus at meiosis. After first nuclear division, the amount is shown as the total amount in the two nuclei. (B) Effect of Fzr1 depletion on changes in nuclear Cdc13-GFP amount at MI. Arrows show disappearance of Cdc13-GFP from the spindle. Gray areas show anaphase determined by Cdc13 disappearance from the spindle and spindle behavior. Time 0 is the start of MI spindle formation. Dotted lines in graphs show boundaries of different meiotic stages.

MI and MII was shortened in *rec12* so that despite the extensive delay in MI execution, MII started with a slight delay after MI initiation (Fig. 3 E, Wt and *rec12*, MII). This may mean that MII is programmed to start at a certain time after MI initiation and somewhat independently of MI completion.

More interestingly, in *rec12*, anaphase II onset was substantially advanced in relation to MII initiation, as shown by the shortening of phase II by ~4 min on average (~26% shortening; Fig. 3 D, *rec12*, phase II, $P < 0.0000005$). This advancement was not specific to this mutant nor caused by expression of GFP-tagged α2-tubulin because phase II shortening was also observed in the *rec7* mutant (unpublished data), and almost identical results were obtained when the spindle dynamics was monitored by a GFP-tagged SPB protein Spo15 (Nakase et al., 2004). Therefore, when the SAC is fully activated at MI, anaphase II onset advances.

We next depleted Clr4 in *rec12* to determine if the MI SAC activation influences the SAC-induced anaphase II delay. In the *rec12* background, Clr4 depletion brought about the anaphase II delay, but the delay was shorter (Fig. 3 D, *rec12* and *rec12 clr4*, phase II); on average, Clr4 depletion extended phase II by 9 min at MII in the *rec12*$^+$ background (Fig. 3 D, Wt and *clr4*) but only by 4.8 min in the *rec12*$^-$ background (Fig. 3 D, *rec12* and *rec12 clrr4*). These results indicate that in the *rec12*$^-$ background, the SAC cannot induce a full level of delay at MII. Thus, in addition to advancement of anaphase onset, the MI SAC activation reduces the SAC effect at MII.

Fzr1 contributes to anaphase initiation and cyclin degradation at meiosis

Why does anaphase II onset advance in *rec12*? One possibility is that reduction of the SAC activity causes the advancement. This possibility is unlikely because the Mad2 depletion alone did not cause any significant advancement of anaphase onset at MII (Fig. 3 D, mad2), although it did at MI ($P < 0.000002$ by *t* test; Fig. 2 C, mad2).

To obtain a clue about the mechanism of the advancement of anaphase II onset, we quantified the amount of Cdc13-GFP in the nucleus by GFP fluorescence intensities and examined its changes during meiotic progression. In *rec12*, timing of Cdc13 decrease was markedly different in relation to anaphase onset, which was judged by spindle elongation and/or disappearance of Cdc13 from the spindle. In the wild-type cells, the nuclear Cdc13 started to decline slightly after anaphase onset at MI (1 min later at MI on average, $n = 9$), and the Cdc13 amount reached the minimal level around the end of anaphase I (Fig. 4 A, Wt). The subsequent Cdc13 reaccumulation started after anaphase I, and Cdc13 again declined around anaphase onset (a mean 0.1 min earlier, $n = 15$; Fig. 4 A, Wt, MII, arrow) and eventually disappeared. In contrast, in *rec12*, despite the marked delay in anaphase onset (Fig. 4 A, *rec12*, MI, arrow), Cdc13 decline was only slightly delayed at MI so that its decline started before anaphase onset (3.7 min earlier, $n = 8$; Fig. 4 A, *rec12*, MI, arrow) and the amount of Cdc13 reached the minimal level before the end of anaphase I. Cdc13 reaccumulated after anaphase I as in the wild type, but the next decline started before anaphase onset at MII (2.2 min earlier, $n = 11$; Fig. 4 A, *rec12*, MII, arrow). Furthermore, the maximal level of Cdc13 at MI and MII and its minimal level after anaphase I were slightly decreased on average (Fig. S1 D). It is currently unclear if this decrease is significant because of the lack of proper internal controls for the GFP signal. mDsRed-tagged α2-tubulin expression did not affect the Cdc13 dynamics, as the same dynamics were observed in cells lacking the GFP-tubulin (Fig. S1 C).

The preanaphase I decrease of Cdc13 in *rec12* raised the possibility that there is another cyclin degradation activity that

is inefficiently inhibited by the SAC; this activity induces preanaphase cyclin degradation at MI and causes advancement of anaphase II onset. To test this possibility, we examined Cdc20-related APC/C activators with a meiosis-specific expression in the fission yeast: Fzr1, a factor previously shown to be required for proper sporulation (Asakawa et al., 2001; Blanco et al., 2001); and Fzr2 (SPAC13G6.08) and Fzr3 (SPCC1620.04c), two factors with unknown functions (Asakawa et al., 2001). We depleted these factors to determine if they contribute to anaphase.

Depletion of either Fzr2 or Fzr3 did not cause any significant changes in anaphase onset (Fig. S2 C, phase II) but significantly shortened the MI–MII interval (Fig. S2 D, interval). Thus, Fzr2 and Fzr3 likely play a role in MII initiation but not in anaphase. In contrast, the Fzr1 depletion, though there were no apparent effects on two divisions or chromosome segregation (not depicted; Asakawa et al., 2001), caused significant extension of phase II at both divisions ($P < 0.05$ at MI and $P < 0.001$ at MII; Figs. 2 C and 3D, *fzr1*, phase II) in addition to shortening of the MI–MII interval (Fig. S2 D, interval). This indicates that Fzr1 participates in anaphase regulation in addition to MII initiation. Fzr1 probably contributes to the anaphase Cdc13 degradation because the Fzr1 depletion delayed the spindle Cdc13 disappearance at both divisions (Fig. S1 B, *fzr1*) and the nuclear Cdc13 decline at MI (the decline starts 4 min after anaphase I onset on average, $n = 7$; Figs. 4 B and S1 C, *fzr1*).

The critical role of Fzr1 in the meiotic progression was further supported by its relationship with a meiosis-specific factor, Mes1, that inhibits APC/C^{Slp1} to initiate MII. MII is not initiated in *mes1* cells, but reduction of the APC/C^{Slp1} activity by an *slp1-362* mutation restores MII in these cells (Izawa et al., 2005). Interestingly, it was also reported that Mes1 inhibits Fzr1 as well as Slp1 from interacting with Cdc13 in vitro. If APC/C^{Fzr1} functions and is inhibited by Mes1 at anaphase I in vivo, the Fzr1 depletion may restore MII in the *mes1* cells, as does the *slp1-362* mutation. We examined this possibility by monitoring the spindle behavior in individual cells. Consistent with previous findings, the majority of the Mes1-lacking cells underwent only MI, and the population of the cells that underwent MI and MII was only ~20% (Fig. 5 A, *mes1*). Introduction of the *slp1-362* mutation restored MII in the Mes1-lacking cells, resulting in an increase in the population to ~60% (Fig. 5 A, *mes1 slp1*). These results support the notion that Mes1 inhibits APC/C^{Slp1} to initiate MII. Importantly, the Fzr1 depletion restored MII more efficiently (Fig. 5 A, *mes1 fzr1*; Izawa, D., and M. Yamamoto, personal communication). These results suggest that Mes1 also inhibits APC/C^{Fzr1} to initiate MII and that APC/C^{Fzr1} degrades Cdc13 at anaphase I. The lower restoration efficiency of *slp1-362* is not caused by metaphase arrest induced by the *slp1-362* mutation because metaphase arrest was eliminated in the *mes1 slp1* cells (Fig. 5 B, meiosis I), and this may rather reflect the remaining weak activity of Slp1 in the *slp1-362* mutant or the distinct role of Slp1 in MII initiation. In the *mes1* background, in addition, the Fzr1 depletion additively delayed anaphase II onset together with the *slp1* mutation (Fig. 5 B, meiosis II), which supports the notion that Fzr1 contributes to anaphase. However, such an effect was not observed at MI (Fig. 5 B, meiosis I). This may mean that contribution of Fzr1 to anaphase is different at MI and MII.

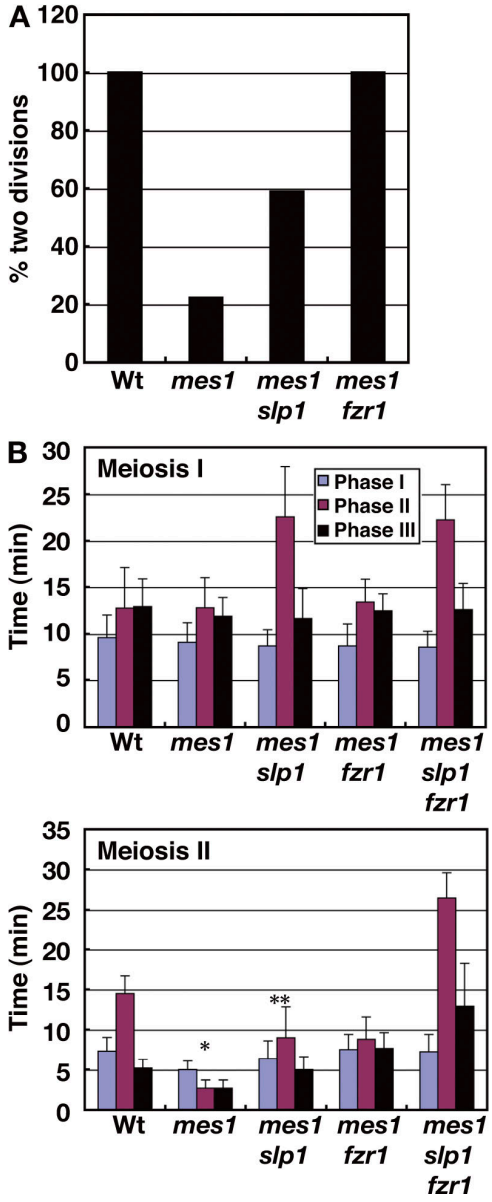

Figure 5. **Functional relationship of Mes1 with Fzr1 and Slp1.** (A) The population of cells that underwent MI and MII. MI and MII were judged by the formation of the MI and MII spindles, respectively. 21, 18, and 17 cells were examined for the wild type, *mes1*, and other mutant strains, respectively. (B) Duration of the spindle phases in the *mes1* mutants. Wt, wild type. *, results of 4 spindles; **, results of 10 spindles. Error bars indicate standard deviation.

Fzr1 advances anaphase II onset in the *rec12* mutant

As Fzr1 contributes to anaphase, we examined if Fzr1 is responsible for the preanaphase cyclin degradation and the advancement of anaphase II onset in *rec12*. The Fzr1 depletion, although it caused no additional delay in anaphase onset (Fig. 2 C, *rec12 fzr1*), delayed nuclear Cdc13 decline at MI in *rec12* (Figs. 4 B and S1 C, *rec12 fzr1*) so that nuclear Cdc13 declined almost concomitantly with anaphase onset (0.3 min after the onset on average, $n = 6$). This indicates that Fzr1 induces the preanaphase Cdc13 decline and suggests that the SAC inhibits Fzr1 inefficiently. Supporting the inefficient inhibition of Fzr1, Fzr1

failed to interact with Mad2, unlike Slp1, in the yeast two-hybrid assay (Fig. S3 A). Remarkably, the Fzr1 depletion delayed the next decline of the nuclear Cdc13 and the disappearance of the spindle Cdc13 at MII (Fig. S1, B and C, *rec12 fzr1*), and completely eliminated the advancement of anaphase II onset in *rec12* (Fig. 3 D, *rec12 fzr1*, phase II). Thus, Fzr1 is responsible for the advancement. The Fzr1 depletion also slightly extended *clr4*-dependent anaphase II delay in the *rec12* background (Fig. 3 D, *rec12 fzr1* and *rec12 clr4 fzr1*; phase II was 6 min longer on average in *rec12 clr4 fzr1* than in *rec12 fzr1*, whereas it is 4.8 min longer in *rec12 clr4* than in *rec12*). Furthermore, unlike Slp1, Fzr1 reduced the SAC-induced metaphase arrest in the *nda3* β-tubulin mutant (Hiraoka et al., 1984) when expressed in mitosis, decreasing the cells with condensed chromosomes and increasing those with decondensed chromosomes significantly (Fig. S3 D). Thus, Fzr1 may contribute to reduction of the SAC-dependent anaphase delay. In summary, these results indicate that Fzr1 probably advances anaphase II onset in the *rec12* mutant.

Discussion

Dynamics of the spindle, the chromosome, and Cdc13 at meiosis

In this study, we elucidated the details of the chromosome and Cdc13 dynamics in relation to the spindle dynamics at meiosis in living fission yeast cells, providing a basis for the analysis of the mechanism of meiotic chromosome segregation. We showed that the spindle elongates in three phases, that chromosomes attach to the spindle during the early stage of spindle elongation and undergo anaphase A and anaphase B, and that Cdc13 disappears from the spindle and decreases in the nucleus around anaphase onset. Concomitant occurrence of the Cdc13 disappearance from the spindle and anaphase spindle elongation supports the idea that cyclin B degradation on the spindle triggers anaphase elongation; degradation of the spindle cyclin probably causes inactivation of Cdk and induces phosphatase-dependent transition of the metaphase spindle to the anaphase spindle, as described for budding yeast mitosis (Higuchi and Uhlmann, 2005). In addition, our observation that disappearance of the nuclear Cdc13 starts from the SPB to the spindle midzone may mean that cyclin degradation occurs from the spindle pole.

We also showed how sister chromatid cohesion is resolved at meiosis, the details of which were previously unclear. At MI, sister chromatids undergo separation solely at the arms, which occurs around anaphase onset. Arm separation, however, does not occur with the same timing along the chromosome length; telomere-proximal regions separate slightly later than other regions, which may mean that telomere disjunction occurs after arm separation. Furthermore, contrary to the general view, arm cohesion is still retained around centromeres at MII. The centromere-proximal arm regions may never undergo dissociation. Alternatively, arm cohesion may be reestablished at the centromere-proximal regions after MI.

Analyses of the *rec12* and *rec8* mutants showed that when chromosomes are prematurely separated before anaphase, they oscillate between the two poles independently of each other and the spindle prematurely elongates, as seen in other organisms (Nicklas, 1961; Severin et al., 2001; Parry et al., 2003). The chromosome oscillation likely reflects repeated cycles of chromosome detachment from one pole and their reattachment to the other pole, whereas the premature spindle elongation is probably caused by a lack of tension at the kinetochore that counteracts with an elongation force. Abnormal MI spindle morphology seen in *rec12* (Fig. 2 B, bottom) is probably caused by elongation of the metaphase spindle whose microtubule dynamics is distinct from that of the anaphase spindle (Mallavarapu et al., 1999; Higuchi and Uhlmann, 2005). Occasional spindle regression may be caused by bipolar attachment of sister kinetochores (in *rec12*) or a single sister kinetochore (in *rec8*). We also showed that although the *clr4* mutant is defective in sister centromere cohesion like the *rec8* mutant, its phenotype is different; independent oscillation of sister chromatids and premature spindle elongation did not occur. Although Clr4 is required for chromosome localization of Rec8, Rec8 may not be completely dislocalized from the chromosome and may loosely hold sister chromatids together in *clr4*.

The SAC delays anaphase onset at meiosis

Our examination of the *rec12* mutant and the *rec8* or *clr4* mutant showed that the SAC delays anaphase onset at both meiotic divisions. This conclusion was drawn from the delay in anaphase events (which include spindle elongation, cyclin degradation, and sister chromatid arm separation) and elimination of this delay by Mad2 depletion. In *rec12*, Mad2 depletion also eliminated abnormal elongation of the MI spindle, probably because the abnormality was the result of SAC-induced delay in metaphase–anaphase transition of the spindle. As in mitosis, the SAC probably inhibits APC/C^{Slp1} because the *slp1-mr63* mutation abolishes the delay. The SAC probably senses a lack of tension at the kinetochore and/or improper spindle attachment of chromosomes because a lack of tension and improper attachments are common in all of the mutants. To our knowledge, this is the first finding that the SAC delays anaphase onset at MII.

Anaphase regulation by the APC/C activators at meiosis

The most important finding of this study is that SAC activation at MI causes advancement of anaphase onset and reduction of the SAC effect at MII; thus, impacts of SAC activation are not confined to a single division at meiosis. We found that Fzr1 depletion largely eliminated this advancement and slightly restored the SAC effect. Furthermore, Fzr1 reduced SAC-induced metaphase arrest in the *nda3* mutant. Given these facts, the most plausible explanation is that Fzr1 induces the advancement and contributes to reduction of the SAC effect, although we cannot exclude a possibility completely that the advancement is caused by an Fzr1-independent mechanism, and Fzr1 depletion eliminated the advancement by merely inducing an additive delay.

Fzr1 is required for sporulation but is dispensable for two divisions (Asakawa et al., 2001; Blanco et al., 2001). However, Fzr1 also contributes to the Cdc13 degradation and anaphase initiation at both divisions, as shown by delayed Cdc13 decline and anaphase onset in Fzr1-lacking cells. The Fzr1 functions are likely conserved among eukaryotes because budding yeast

Ama1 is also dispensable for two divisions and contributes to the degradation of APC/C substrates and anaphase I progression (Cooper et al., 2000; Oelschlaegel et al., 2005; Penkner et al., 2005). Fzr1 is probably inefficiently inhibited by the SAC because Fzr1 induces preanaphase Cdc13 decline at MI in *rec12* and fails to interact with Mad2 in the yeast two-hybrid assay. Furthermore, the Fzr1 contribution may be greater at MII than at MI because Fzr1 depletion delayed anaphase initiation at MII but not at MI in the *mes1* background (Fig. 5 B). This may account for the undetectable effects of the Mad2 depletion on anaphase II onset and normal morphology of the prematurely elongated MII spindle in *rec8*.

Fzr1 apparently regulates anaphase together with Slp1, a central regulator of anaphase (Fig. S2, A and B; Izawa et al., 2005). We speculate that a major role of Fzr1 is to help Slp1 to execute anaphase swiftly. Perhaps Fzr1 confers the substrate specificity on APC/C, which is largely overlapping with that of Slp1, but is more preferential for anaphase completion rather than anaphase initiation, such that Fzr1 alone can hardly induce anaphase. Fzr1 probably also functions after MI to ensure exit from anaphase I and thereby delays initiation of the next division.

Considering the supportive role of Fzr1, the function of Fzr1 may be similar to that of Cdh1 in mitosis (Peters, 2006). Consistently, Fzr1 is most similar to Ste9/Srw1 (fission yeast Cdh1) in sequence (Asakawa et al., 2001), and not only Fzr1, but also budding yeast Cdh1, is inefficiently inhibited by the SAC (Ushimaru, T., personal communication). One idea is that Fzr1 replaces Ste9/Cdh1 at meiosis. Given shortening of the MI–MII interval in *rec12*, there is probably a meiosis-specific regulatory mechanism that induces MII events with certain timings after MI initiation. This mechanism is perhaps required to execute two consecutive divisions and/or prevent DNA replication, and a replacement of Ste9/Cdh1 by Fzr1 may be inevitable for the mechanism to accomplish its task. At present, it is known that Ste9/Cdh1 is dispensable for execution of two meiotic divisions in both budding and fission yeasts (unpublished data; Buonomo et al., 2003) and that it is required for entry into meiosis from G1 in fission yeast (Kitamura et al., 1998; Yamaguchi et al., 1997), but, otherwise, the meiotic functions of Ste9/Cdh1 remain unclear. Future studies will be required to elucidate the precise meiotic roles of both Fzr1 and Cdh1/Ste9.

A meiotic regulatory mechanism that induces advancement of anaphase II onset

It is apparent that MI SAC activation causes advancement of anaphase II onset by advancing APC/C^{Slp1} activation, as APC/C^{Slp1} is a major initiator of anaphase and the SAC can delay anaphase II in *rec12* despite the advancement. However, how MI SAC activation advances APC/C^{Slp1} activation remains unclear. As shown by Cdc13 analysis, APC/C^{Fzr1} induces preanaphase I degradation of APC/C substrates in *rec12*. One possibility is that preanaphase I degradation of critical meiotic regulators induced by APC/C^{Fzr1} advances APC/C^{Slp1} activation at MII. Because the SAC inhibition of APC/C^{Slp1} is likely incomplete, as suggested by a limited period of MI delay in *rec12*, APC/C^{Slp1} that escapes from the inhibition may also contribute to the preanaphase I degradation. An alternative but not mutually exclusive possibility is that delayed MI activation of APC/C^{Slp1} and/or shortening of the MI–MII interval alters accumulation levels of critical meiotic regulators and causes activation of APC/C^{Fzr1} in an untimely manner, which in turn causes advancement of APC/C^{Slp1} activation. The altered accumulation of the regulators may also contribute to advancement of APC/C^{Slp1} activation independently of APC/C^{Fzr1}. In this possibility, SAC-independent MI delay may also cause the advancement. In any scenarios, Mes1 may play a critical role in the advancement because it negatively regulates both APC/C^{Slp1} and APC/C^{Fzr1} to induce MII and is itself an APC/C substrate (Fig. 5; Izawa et al., 2005; Kimata et al., 2008).

The reason for the SAC effect reduction is also unclear. Duration of the SAC effect may be limited at meiosis. Alternatively, there may be an adaptation mechanism that reduces the SAC effect after MI SAC activation. APC/C^{Fzr1} may contribute to the reduction by degrading SAC factors, as some SAC factors were shown to be the APC/C substrates (Palframan et al., 2006; Qi and Yu, 2007).

It is possible that the advancement of anaphase onset is a general phenomenon of anaphase, and anaphase onset may advance during mitosis when the SAC delays the previous division. However, we favor an idea that the advancement is meiosis specific because the advancement depends on a meiosis-specific APC/C activator, and meiotic anaphase regulation is substantially different. The regulatory mechanism that induces the advancement is perhaps common among eukaryotes, as Fzr1 functions are likely conserved between two evolutionally divergent yeasts and have likely been evolved for execution of two consecutive divisions. It may not be able to afford substantial SAC activation or progression delay, and the advancement may be a consequence of perturbed meiotic progression that resulted from the MI SAC activation or delay. Alternatively, the mechanism may have been evolved not only for two divisions but also for swift completion of meiosis, and the advancement may be actively induced by it. Swift completion of meiosis may be advantageous for organisms that produce a large amount of gametes such as sperms in a relatively short period, and especially for those which undergo meiosis in nutrient-poor conditions, like yeasts, because it would increase chances for the cells to generate gametes before using up the nutrients.

Our finding may be clinically important. In human meiosis, trisomy that leads to abortion or mental retardation originates from chromosome missegregation at both MI and MII (Hassold and Hunt, 2001). The MI defect-dependent advancement of anaphase II onset may partly account for such divergent origins of human trisomy in spermatogenesis in which meiosis progresses without arrests, as in fission yeast. The advancement of anaphase II onset apparently increases the chance of chromosome missegregation at MII by reducing the time for establishing spindle attachment of chromosomes and correcting improper attachments. This means that the outcome of an MI hazardous event may be divergent; it can cause chromosome missegregation not only at MI but also at MII. Eukaryotic organisms have evolved a mechanism that executes two meiotic divisions swiftly but may in turn have assumed the risk of chromosome missegregation.

Materials and methods

Yeast strains and media

Fission yeast strains used in this study are shown in Table S1. Media for fission yeast are described in Moreno et al. (1991). Yeast extract peptone dextrose medium contained 1% yeast extract, 2% polypeptone, and 2% glucose. The budding yeast strain used in the two-hybrid assay was PJ69-4A (a gift from T. Ushimaru, Shizuoka University, Shizuoka, Japan; James et al., 1996).

Construction of cells expressing α2-tubulin tagged with monomeric DsRed

A DNA fragment encoding the *atb2*$^+$ gene and the *nmt1* terminator was amplified by PCR using synthetic oligonucleotide primers (5′-CGGGATCCATGAGAGAGATCATTTCCATTCA-3′ and 5′-GAATTCGAGCTCGCATTACTAATA-3′) and plasmid pDQ105 as a template. The fragment was digested with BamHI and SacI and then inserted between the BglII and SacI sites of an integration plasmid, p1095, which bears a gene encoding monomeric DsRed (a gift from Y. Chikashige, Kansai Advanced Research Center, National Institute of Information and Communications Technology, Kobe, Japan), generating the fusion gene of mDsRed and α2-tubulin. The DNA fragment containing the *nda3* promoter was then amplified by PCR using synthetic oligo nucleotide primers (5′-GAAGATCTCATATATGCCGTATTCTTGAATG-3′ and 5′-GAAGATCTAGACTAATTTATGGTGGTTTGT-3′). The amplified fragment was digested by BglII and inserted at the BamHI site of the plasmid bearing the fusion gene such that the fusion gene expression was driven by the *nda3* promoter. The resultant plasmid was transformed into cells bearing *lys1-131*. The integrants were selected by *lys1*$^+$ phenotype, and their integration was confirmed by colony PCR.

Live cell analysis of spindle and chromosome dynamics

Cells were grown on solid YES medium at 33°C and then induced to undergo meiosis by incubation on solid ME medium for 12–16 h. The cells were then suspended in EMM medium lacking nitrogen and observed for dynamics of the GFP-labeled spindle or chromosomes at 26°C as described previously (Yamamoto et al., 2001; Ding et al., 2006). A computer-controlled microscope system including the objective lens and camera is described in Ding et al. (2006). Chromosome or spindle behavior was observed every 1 or 2 min, respectively. A set of images from six focal planes at 0.5-μm intervals was taken at each time point. The measurements were conducted in three dimensions. In each analysis of the spindle, at least 15 spindles were examined if not indicated.

Quantification of fluorescence intensity of Cdc13-GFP

A quantitative analysis of the GFP signals was performed as described previously (Ding et al., 2006). A set of images of cells expressing Cdc13-GFP was taken every 2 min as described for analysis of spindle and chromosome dynamics. Each set of images was processed by deconvolution using the SoftWoRx software on the DeltaVision system (Applied Precision, LLC). The processed images were combined to form a quantitative projection using an additive image projecting method. On the projections, the 2D polygons were drawn for the nuclear Cdc13-GFP, and the sums of the fluorescence intensities in the polygons were obtained. When GFP was not detected at the MI–MII transition, the 2D polygons were inferred from the images taken at previous time points.

Online supplemental material

Fig. S1 shows timing of Cdc13-GFP disappearance from the spindle and the level of Cdc13-GFP in the nucleus. Fig. S2 shows roles of APC/C activators in the progression of meiosis. Fig. S3 shows Mad2 localization, its functional relationship with APC/C activators, and MII spindle dynamics in the *rec12* mutant. Table S1 shows the strains used in this study and their source. Table S2 shows parameters of meiotic centromere movements in various strains. Online supplemental material is available at http://www.jcb.org/cgi/content/full/jcb.200802053/DC1.

We thank Daisuke Izawa, Masayuki Yamamoto, and Takashi Ushimaru for sharing unpublished results. We thank Mitsuhiro Yanagida, Takashi Toda, Tomohiro Matsumoto, Yoshinori Watanabe, Kathleen Gould, Osami Niwa, Jun-ichi Nakayama, Hirohisa Masuda, Haruhiko Asakawa, Chikashi Shimoda and Monika Molnar for strains, Yuji Chikashige and Takashi Ushimaru for strains and reagents, Da-Qiao Ding for advice on quantification of Cdc13-GFP, Toshiyuki Hatano and Hironori Niki for use of the Delta Vision microscope system, and Roger Tsien for the monomeric DsRed construct. We also thank Orna Cohen-Fix, Alexander Strunnikov, Masahiro Uritani, and Takashi Ushimaru for critical reading of the manuscript and helpful comments. Some strains used in this study were provided by the Yeast Genetic Resource Center Japan. Some results were obtained using instruments at the Center for Instrumental Analysis and Institute for Genetic Research and Biotechnology at Shizuoka University.

This work was supported by National Institute of Genetics Cooperative Research Program 2007-A68, Grants-in-Aid for Scientific Research on Priority Areas and Scientific Research (C) (16570169) from the Ministry of Education, Culture, Sports, Science and Technology of Japan (to A. Yamamoto), and grants from the Japan Science and Technology Agency Corporation (to Y. Hiraoka).

Submitted: 11 February 2008
Accepted: 23 June 2008

References

Asakawa, H., K. Kitamura, and C. Shimoda. 2001. A novel Cdc20-related WD-repeat protein, Fzr1, is required for spore formation in *Schizosaccharomyces pombe*. *Mol. Genet. Genomics.* 265:424–435.

Blanco, M.A., L. Pelloquin, and S. Moreno. 2001. Fission yeast mfr1 activates APC and coordinates meiotic nuclear division with sporulation. *J. Cell Sci.* 114:2135–2143.

Buonomo, S.B., K.P. Rabitsch, J. Fuchs, S. Gruber, M. Sullivan, F. Uhlmann, M. Petronczki, A. Toth, and K. Nasmyth. 2003. Division of the nucleolus and its release of CDC14 during anaphase of meiosis I depends on separase, SPO12, and SLK19. *Dev. Cell.* 4:727–739.

Cervantes, M.D., J.A. Farah, and G.R. Smith. 2000. Meiotic DNA breaks associated with recombination in *S. pombe*. *Mol. Cell.* 5:883–888.

Cohen-Fix, O., J.M. Peters, M.W. Kirschner, and D. Koshland. 1996. Anaphase initiation in *Saccharomyces cerevisiae* is controlled by the APC-dependent degradation of the anaphase inhibitor Pds1p. *Genes Dev.* 10:3081–3093.

Cooper, K.F., M.J. Mallory, D.B. Egeland, M. Jarnik, and R. Strich. 2000. Ama1p is a meiosis-specific regulator of the anaphase promoting complex/cyclosome in yeast. *Proc. Natl. Acad. Sci. USA.* 97:14548–14553.

D'Amours, D., and A. Amon. 2004. At the interface between signaling and executing anaphase–Cdc14 and the FEAR network. *Genes Dev.* 18:2581–2595.

Decottignies, A., P. Zarzov, and P. Nurse. 2001. In vivo localisation of fission yeast cyclin-dependent kinase cdc2p and cyclin B cdc13p during mitosis and meiosis. *J. Cell Sci.* 114:2627–2640.

Ding, D.Q., A. Yamamoto, T. Haraguchi, and Y. Hiraoka. 2004. Dynamics of homologous chromosome pairing during meiotic prophase in fission yeast. *Dev. Cell.* 6:329–341.

Ding, D.Q., N. Sakurai, Y. Katou, T. Itoh, K. Shirahige, T. Haraguchi, and Y. Hiraoka. 2006. Meiotic cohesins modulate chromosome compaction during meiotic prophase in fission yeast. *J. Cell Biol.* 174:499–508.

Funabiki, H., H. Yamano, K. Kumada, K. Nagao, T. Hunt, and M. Yanagida. 1996. Cut2 proteolysis required for sister-chromatid separation in fission yeast. *Nature.* 381:438–441.

Hassold, T., and P. Hunt. 2001. To err (meiotically) is human: the genesis of human aneuploidy. *Nat. Rev. Genet.* 2:280–291.

Higuchi, T., and F. Uhlmann. 2005. Stabilization of microtubule dynamics at anaphase onset promotes chromosome segregation. *Nature.* 433:171–176.

Hiraoka, Y., T. Toda, and M. Yanagida. 1984. The NDA3 gene of fission yeast encodes beta-tubulin: a cold-sensitive nda3 mutation reversibly blocks spindle formation and chromosome movement in mitosis. *Cell.* 39:349–358.

Huang, J., and J.W. Raff. 1999. The disappearance of cyclin B at the end of mitosis is regulated spatially in *Drosophila* cells. *EMBO J.* 18:2184–2195.

Iwabuchi, M., K. Ohsumi, T.M. Yamamoto, W. Sawada, and T. Kishimoto. 2000. Residual Cdc2 activity remaining at meiosis I exit is essential for meiotic M-M transition in *Xenopus* oocyte extracts. *EMBO J.* 19:4513–4523.

Izawa, D., M. Goto, A. Yamashita, H. Yamano, and M. Yamamoto. 2005. Fission yeast Mes1p ensures the onset of meiosis II by blocking degradation of cyclin Cdc13p. *Nature.* 434:529–533.

Jacobs, H., D. Richter, T. Venkatesh, and C. Lehner. 2002. Completion of mitosis requires neither fzr/rap nor fzr2, a male germline-specific *Drosophila* Cdh1 homolog. *Curr. Biol.* 12:1435–1441.

James, P., J. Halladay, and E.A. Craig. 1996. Genomic libraries and a host strain designed for highly efficient two-hybrid selection in yeast. *Genetics.* 144:1425–1436.

Kim, S.H., D.P. Lin, S. Matsumoto, A. Kitazono, and T. Matsumoto. 1998. Fission yeast Slp1: an effector of the Mad2-dependent spindle checkpoint. *Science.* 279:1045–1047.

Kimata, Y., M. Trickey, D. Izawa, J. Guannon, M. Yamamoto, and H. Yamano. 2008. A mutual inhibition between APC/C and its substrate Mes1 required for meiotic progression in fission yeast. *Dev. Cell.* 14:446–454.

Kitajima, T.S., S. Yokobayashi, M. Yamamoto, and Y. Watanabe. 2003. Distinct cohesin complexes organize meiotic chromosome domains. *Science.* 300:1152–1155.

Kitamura, K., H. Maekawa, and C. Shimoda. 1998. Fission yeast Ste9, a homolog of Hct1/Cdh1 and Fizzy-related, is a novel negative regulator of cell cycle progression during G1-phase. *Mol. Biol. Cell.* 9:1065–1080.

Lin, Y., and G.R. Smith. 1994. Transient, meiosis-specific expression of the *rec6* and *rec12* genes of *Schizosaccharomyces pombe. Genetics.* 136:769–779.

Mallavarapu, A., K. Sawin, and T. Mitchison. 1999. A switch in microtubule dynamics at the onset of anaphase B in the mitotic spindle of *Schizosaccharomyces pombe*. *Curr. Biol.* 9:1423–1426.

Moreno, S., A. Klar, and P. Nurse. 1991. Molecular genetic analysis of fission yeast *Schizosaccharomyces pombe. Methods Enzymol.* 194:795–823.

Musacchio, A., and K.G. Hardwick. 2002. The spindle checkpoint: structural insights into dynamic signalling. *Nat. Rev. Mol. Cell Biol.* 3:731–741.

Nabeshima, K., T. Nakagawa, A.F. Straight, A. Murray, Y. Chikashige, Y. Yamashita, Y. Hiraoka, and M. Yanagida. 1998. Dynamics of centromeres during metaphase-anaphase transition in fission yeast: dis1 is implicated in force balance in metaphase bipolar spindle. *Mol. Biol. Cell.* 9:3211–3225.

Nakase, Y., T. Nakamura, K. Okazaki, A. Hirata, and C. Shimoda. 2004. The Sec14 family glycerophospholipid-transfer protein is required for structural integrity of the spindle pole body during meiosis in fission yeast. *Genes Cells.* 9:1275–1286.

Nicklas, R.B. 1961. Recurrent pole-to-pole movements of the sex chromosome during prometaphase I in *Melanoplus differentialis* spermatocytes. *Chromosoma.* 12:97–115.

Nicklas, R.B. 1997. How cells get the right chromosomes. *Science.* 275:632–637.

Oelschlaegel, T., M. Schwickart, J. Matos, A. Bogdanova, A. Camasses, J. Havlis, A. Shevchenko, and W. Zachariae. 2005. The yeast APC/C subunit Mnd2 prevents premature sister chromatid separation triggered by the meiosis-specific APC/C-Ama1. *Cell.* 120:773–788.

Palframan, W.J., J.B. Meehl, S.L. Jaspersen, M. Winey, and A.W. Murray. 2006. Anaphase inactivation of the spindle checkpoint. *Science.* 313:680–684.

Parry, D.H., G.R. Hickson, and P.H. O'Farrell. 2003. Cyclin B destruction triggers changes in kinetochore behavior essential for successful anaphase. *Curr. Biol.* 13:647–653.

Penkner, A.M., S. Prinz, S. Ferscha, and F. Klein. 2005. Mnd2, an essential antagonist of the anaphase-promoting complex during meiotic prophase. *Cell.* 120:789–801.

Peters, J.M. 2006. The anaphase promoting complex/cyclosome: a machine designed to destroy. *Nat. Rev. Mol. Cell Biol.* 7:644–656.

Petronczki, M., M.F. Siomos, and K. Nasmyth. 2003. Un menage a quatre: the molecular biology of chromosome segregation in meiosis. *Cell.* 112:423–440.

Qi, W., and H. Yu. 2007. KEN-box-dependent degradation of the Bub1 spindle checkpoint kinase by the anaphase-promoting complex/cyclosome. *J. Biol. Chem.* 282:3672–3679.

Severin, F., A.A. Hyman, and S. Piatti. 2001. Correct spindle elongation at the metaphase/anaphase transition is an APC-dependent event in budding yeast. *J. Cell Biol.* 155:711–718.

Shonn, M.A., R. McCarroll, and A.W. Murray. 2000. Requirement of the spindle checkpoint for proper chromosome segregation in budding yeast meiosis. *Science.* 289:300–303.

Skibbens, R.V., V.P. Skeen, and E.D. Salmon. 1993. Directional instability of kinetochore motility during chromosome congression and segregation in mitotic newt lung cells: a push-pull mechanism. *J. Cell Biol.* 122:859–875.

Tomlin, G.C., J.L. Morrell, and K.L. Gould. 2002. The spindle pole body protein Cdc11p links Sid4p to the fission yeast septation initiation network. *Mol. Biol. Cell.* 13:1203–1214.

Watanabe, Y., and P. Nurse. 1999. Cohesin Rec8 is required for reductional chromosome segregation at meiosis. *Nature.* 400:461–464.

Yamaguchi, S., H. Murakami, and H. Okayama. 1997. A WD repeat protein controls the cell cycle and differentiation by negatively regulating Cdc2/B-type cyclin complexes. *Mol. Biol. Cell.* 8:2475–2486.

Yamaguchi, S., A. Decottignies, and P. Nurse. 2003. Function of Cdc2p-dependent Bub1p phosphorylation and Bub1p kinase activity in the mitotic and meiotic spindle checkpoint. *EMBO J.* 22:1075–1087.

Yamamoto, A., and Y. Hiraoka. 2003. Monopolar spindle attachment of sister chromatids is ensured by two distinct mechanisms at the first meiotic division in fission yeast. *EMBO J.* 22:2284–2296.

Yamamoto, A., V. Guacci, and D. Koshland. 1996. Pds1p, an inhibitor of anaphase in budding yeast, plays a critical role in the APC and checkpoint pathway(s). *J. Cell Biol.* 133:99–110.

Yamamoto, A., C. Tsutsumi, H. Kojima, K. Oiwa, and Y. Hiraoka. 2001. Dynamic behavior of microtubules during dynein-dependent nuclear migrations of meiotic prophase in fission yeast. *Mol. Biol. Cell.* 12:3933–3946.